Fractal rock slope dynamics anticipating a collapse

Milan Paluš,[1] Dagmar Novotná,[2] and Jiří Zvelebil[3]
[1]*Institute of Computer Science, Academy of Sciences of the Czech Republic, Pod vodárenskou věží 2, 182 07 Prague 8, Czech Republic*
[2]*Institute of Atmospheric Physics, Academy of Sciences of the Czech Republic, Boční II/1401, 141 31 Prague 4, Czech Republic*
[3]*Institute of Rock Structure and Mechanics, Academy of Sciences of the Czech Republic, V Holešovičkách 41, 182 09 Prague 8, Czech Republic*
(Received 4 April 2003; revised manuscript received 29 April 2004; published 27 September 2004)

Time series of dilatometric measurements of relative displacements on rock cracks on stable and unstable sandstone slopes were analyzed. The inherent dynamics of rock slopes lack any significant nonlinearity. However, the residuals obtained by removing meteorological influences are fat-tailed non-Gaussian fluctuations, with short-range correlations in the case of stable slopes. The fluctuations of unstable slopes exhibit self-affine dynamics of fractional Brownian motions with power-law long-range correlations and are characterized by asymptotic power-law probability distributions with decay coefficients outside the range of stable Lévy distributions.

DOI: 10.1103/PhysRevE.70.036212 PACS number(s): 05.45.Tp, 05.45.Df, 05.40.-a

I. INTRODUCTION

Characteristic features observed in the temporal development of slope movement activity were proposed for evaluation of rock slope stability in 1968 by Bjerrum and Jorstadt in order to overcome the shortcomings of static models [1]. Since then this observational method has been successfully applied for short-term prediction of rock slope collapses with prediction horizons ranging from days to weeks (see [2] and references therein). Zvelebil and Moser have recently demonstrated a successful prediction of a sandstone rock wall collapse two months beforehand [2]. Moreover, they also show examples where the slope dynamics seems to bear predictive information about a possible collapse one or more years in advance. This long-term prediction, however, was based on rather subjective evaluation by experienced experts of qualitative features observed in long-term monitoring of slope movements. If such long-term predictive information exists in the slope movements records, it would be desirable to find an objective, quantitative method for its extraction and evaluation. Zvelebil observed complex hierarchical patterns in long-term slope movement records and proposed to analyze them using modern methods developed in the theory of nonlinear dynamics and deterministic chaos [3–5]. Qin *et al.* recently described landslide evolution using a nonlinear dynamical model exhibiting chaotic behavior [6]. Lyapunov exponents, predictable time scales, and stability criteria were evaluated using this model, which was estimated from the observed landslide data [6].

In this paper, rock slope dynamics, registered as time series of dilatometric measurement of relative displacements on rock cracks, are analyzed. A series of nonlinearity tests is performed using raw and preprocessed data registered at stable and unstable sandstone slopes. Relations between slope movements and dynamics of meteorological variables are also tested. Atmospheric variability and seasonality explain a large portion of slope movement variance. The response to the atmospheric driving as well as the inherent dynamics of rock slopes lack any significant nonlinearity, so any hypothesis of the presence of chaotic dynamics would be unfounded. The inherent slope dynamics, however, are far from being trivial noninformative noise. The residuals obtained from the slope movement series by removing meteorological influences are fat-tailed non-Gaussian fluctuations, with short-range correlations in the case of stable slopes. The fluctuations of unstable slopes exhibit self-affine dynamics of fractional Brownian motions with power-law long-range correlations and are characterized by an asymptotic power-law probability distribution with a decay coefficient outside the range of stable Lévy distributions.

The analyzed data are described in Sec. II. Section III describes the preprocessing of the data, separation of the atmospheric variability reflected in the slope dynamics, and the nonlinearity tests used for testing the hypothesized nonlinearity in the slope movement dynamics and their relations to dynamics of meteorological variables. Distribution and correlation properties of the residuals after removal of atmospheric influences are analyzed in Sec. IV by using standard methods such as estimation of histograms and periodograms, as well as by using the detrended fluctuation analysis [7]. The results are discussed and conclusion given in Sec. V.

II. DATA

Displacements of rock masses—mainly crack openings—were measured by rod dilatometers on kinematically and functionally defined key sites of unstable and potentially unstable rock objects and parts of sandstone rock walls with heights ranging from 40 to 100 m. The sites form a safety monitoring net above the main road to the Czech Republic–Germany border crossing point Hřensko-Schmilka near the city of Děčín. The total length of the net is over 12 km, and with more than 400 measuring sites it covers 100 rock objects [3–5]. Irregularly registered measurements form time series with sampling times ranging from a few days to approximately two weeks. The available time series span the period from January 1984 (or November 1995) to June 2000,

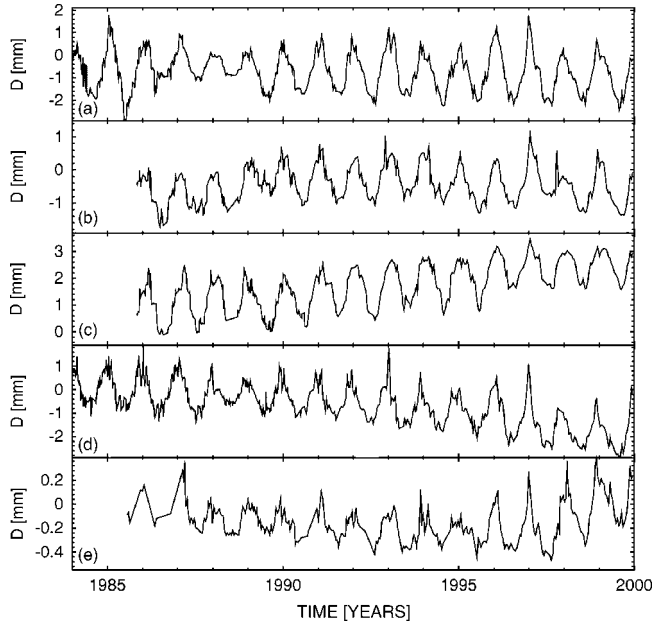

FIG. 1. Time series of dilatometric measurements of relative displacements on rock cracks on stable (a)-(c) and unstable (d), (e) sandstone slopes.

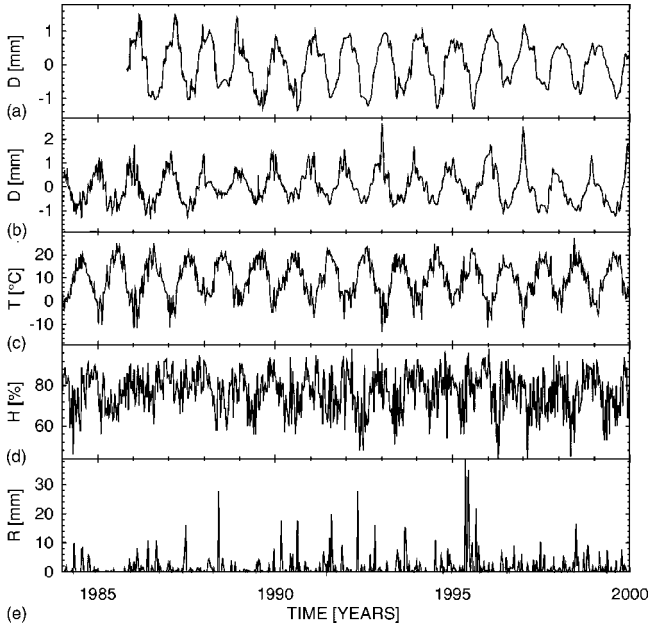

FIG. 2. Linearly detrended time series of dilatometric measurements of relative displacements on rock cracks on stable (a) and unstable (b) sandstone slopes. Time series of atmospheric temperature (c), humidity (d), and precipitation (e) in the region.

thus producing series of lengths from 480 to 612 samples. An engineering geology expert divided the available, large collection of time series into two groups. "Stable series" were obtained from slopes where no patterns signaling danger of a rapid slope collapse have been identified, despite some of the monitored slopes exhibiting irreversible, long-lasting movements. The "unstable series" were recorded on slopes which recently either collapsed or were blasted down after being assessed as approaching a collapse stage. After careful sorting of the data, the majority of recordings were excluded due to incompleteness (large gaps in recordings) and the remaining four unstable and five stable series were analyzed. The examples of the raw data are presented in Fig. 1 [Figs. 1(a)–1(c), stable; Figs. 1(d) and 1(e), unstable series]. Since most time series analysis methods require a regular sampling, the series were resampled by a linear interpolation using a procedure in a time series software package [8]. The 1024 samples obtained were used in further analyses. In parallel, a nonlinearity test for unevenly sampled data [9] was also applied to the raw data.

Some of the time series [both stable, Figs. 1(c), and unstable, Fig. 1(d)] contain a long-term linear trend. Such a clear nonstationarity could influence analyses and therefore the series were linearly detrended [8]. The linearly detrended time series [Figs. 2(a) and 2(b)] can still contain slow nonlinear trends. It is not clear *a priori*, however, whether such nonlinear trends are a part of the dynamics of interest, or should also be removed. Therefore two versions of detrended time series were used in subsequent analysis: linearly detrended, such as the examples in Figs. 2(a) and 2(b); and high-pass filtered series in which frequencies over 1.3 cycle/yr were removed. Spectral as well as time-domain filters [8] were tested and similar results were obtained.

The dynamics of the series are dominated by an annual cycle probably caused by atmospheric influences, mainly by the temperature [3]. Thus the atmospheric variables should be considered in the analyses. Since time series of meteorological data [atmospheric temperature, Fig. 2(c), humidity, Fig. 2(d), and precipitation, Fig. 2(e)] were not measured simultaneously on the same sites as the dilatometric data, they were obtained by concatenating records from the two nearest meteorological stations in the region, Děčín and Ústí nad Labem. Thus we have obtained complete daily data spanning the studied period. For each dilatometric record, time series of the meteorological data with the same sampling were constructed and resampled in the same way as the dilatometric data. We realize that the meteorological data, especially the amounts of precipitation, are characterized by a high spatial variability, so we should use these data cautiously.

III. TESTING FOR NONLINEARITY

The test for nonlinearity in univariate [10] and multivariate data [11] operates with information-theoretic tools [12] such as the well-known mutual information $I(X;Y)$ of two random variables X and Y, given as $I(X;Y)=H(X)+H(Y)-H(X,Y)$, where the entropies $H(X)$, $H(Y)$, and $H(X,Y)$ are given in the usual Shannonian sense [12]. Now, let the variables X and Y have zero means, unit variances, and correlation matrix $\mathbf{C}$. Then, we define a linear version of the mutual information as $L(X;Y)=-(1/2)(\log\sigma_1+\log\sigma_2)$, where σ_i are the eigenvalues of the correlation matrix $\mathbf{C}$.

If the variables X,Y have a two-dimensional Gaussian distribution, then $L(X;Y)$ and $I(X;Y)$ are theoretically equivalent. The general mutual information I detects all dependences in the data under study, while the linear L is sen-

sitive only to linear structures (see [10] and references therein). The test used is based on the so-called surrogate-data [13] approach, in which one computes a *nonlinear* statistic (here I) from the data under study and from an ensemble of realizations of a linear stochastic process, which mimics the "linear properties" of the studied data. If the computed statistic for the original data is significantly different from the values obtained for the surrogate set, one can infer that the data were not generated by a linear process. For the purpose of such tests the surrogate data must preserve the spectrum and consequently, the autocorrelation function of the series under study [13]. (Also, preservation of the histogram is usually required. A histogram transformation used for this purpose is described in [10] and references therein.) In the multivariate case cross correlations between all pairs of variables must also be preserved [14].

As in [10] we define the test statistic as the difference between the mutual information $I(X;Y)$ obtained for the original data and the mean $I(X;Y)$ of a set of surrogates, in the number of standard deviations (SD's) of the latter. The result is considered significant if the difference is clearly larger than two SD's. In this study we applied the univariate version $\boldsymbol{I(}X(t);X(t+\tau)\boldsymbol{)}$ when dynamical properties and nonlinearity of individual series (variables) were studied, and the bivariate version $\boldsymbol{I(}X(t);Y(t+\tau)\boldsymbol{)}$ when dynamical relations between two variables were investigated. The mutual information $I(X;Y)$[o] from the scrutinized data and the mean mutual information $I(X;Y)$[s] from the surrogates, as well as the test statistics, defined above, were plotted as functions of the lag τ. Significant differences found between $I(X;Y)$[o] and $I(X;Y)$[s] were used to infer nonlinearity in the dynamics of a variable (in the univariate case), or in a relation between two variables (in the bivariate case). The same tests as those using the (nonlinear) mutual information $I(X;Y)$ were done with its linear version $L(X;Y)$. Since the latter measures only linear relations in the data, any significance obtained using $L(X;Y)$ indicates imperfect surrogate data. In such cases the significant results obtained using $I(X;Y)$ should be assessed carefully, since they can reflect just a flaw in the surrogates, and the tested data could be linear.

A typical result of the above described testing approach can be seen in Fig. 3, where the relation between the atmospheric temperature and the detrended unstable dilatometric time series is studied. The mutual information $\boldsymbol{I(}X(t);Y(t+\tau)\boldsymbol{)}$ detects a strong periodically changing dependence which seems to be stronger in the data than it is in the linear surrogates [Fig. 3(b)]. This deviation is reflected in statistically significant differences reaching over four SD's [Fig. 3(d)]. A conclusion that the data are nonlinear is prevented by the results from the linear statistic based on the linear redundancy $\boldsymbol{L(}X(t);Y(t+\tau)\boldsymbol{)}$. It also discovers significant differences between the data and the surrogates, i.e., the surrogates do not exactly preserve the linear properties of the data.

Similar results have also been obtained in tests for nonlinearity in relations between the other meteorological variables and the dilatometric data and in testing the dilatometric data themselves.

The fact that surrogates of strongly cyclic data can be flawed has been observed and described (see, e.g., [10] and references therein). One can use more sophisticated (and computationally costly) methods for construction of better surrogate data [15], or try to remove the cyclic component from the studied data. Since an atmospheric source of this annual cyclicity in the studied data can be expected, in the following we fit a multivariate linear regression [8] using the meteorological data as independent variables and the dilatometric series as the dependent variable. The maxima of mutual information between the atmospheric variables and the dilatometric series are located at zero lag, so series without lagging are used in this first series of regressions. The regression residuals are used in further analyses. The results of nonlinearity tests of the residuals are similar to those in Fig. 3, but the dependence is weaker, i.e., the annual cycle was removed only partially. The relation between the residuals and the atmospheric temperature can be seen in Fig. 4. Practically, all the above conclusions hold, only the maximum of $\boldsymbol{I(}X(t);Y(t+\tau)\boldsymbol{)}$ is now in the lag 17 samples. Therefore another linear regression, now with a lagged temperature series, was performed twice—first with the lag 17 samples and then with the lag 21 samples. Residuals of all dilatometric series regressed on meteorological variables were twice more regressed on lagged temperature series with lags determined from such analyses as presented in Fig. 4. These triple regressions finally removed the annual cycle, and in a majority of the stable dilatometric series also any formal nonlinearity (significance in the nonlinearity tests). The results of nonlinearity analysis of the residuals from the triple regression for one of the unstable dilatometric series are presented in Fig.

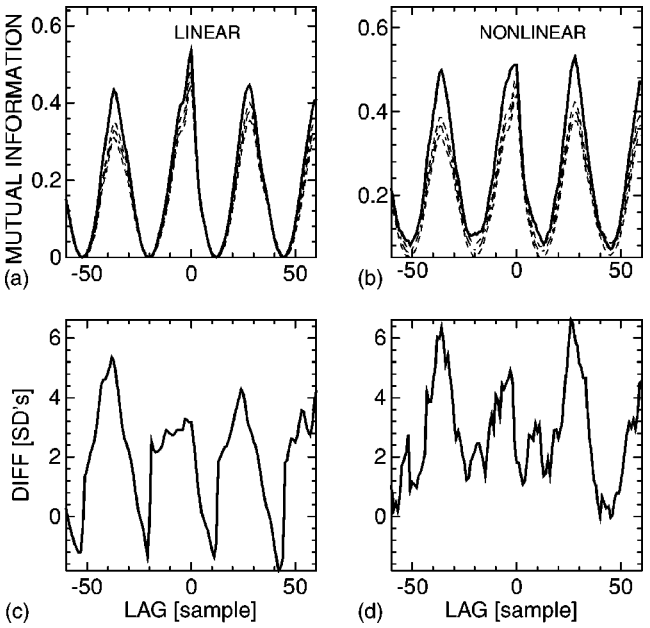

FIG. 3. Testing for nonlinearity in the relationship between atmospheric temperature and the detrended unstable dilatometric time series using mutual information $I(X(t);Y(t+\tau))$ (b), (d) and the check of the surrogate data using linear mutual information $L(X(t);Y(t+\tau))$ (a), (c). The values of mutual information (a,b) from the tested data (solid line), mean (dash-dotted line), and mean ±SD (dashed lines) of a set of 30 realizations of the surrogate data. The statistics, differences in number of standard deviations of the surrogates (c), (d).

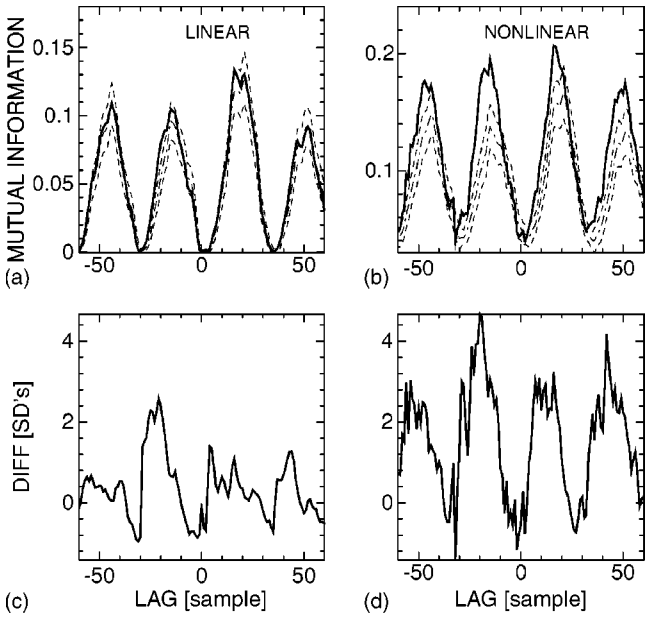

FIG. 4. Testing for nonlinearity in the relationship between atmospheric temperature and the residuals of the multilinear regression of the detrended unstable dilatometric time series on the meteorological variables, using mutual information $I(X(t);Y(t+\tau))$ (b),(d) and the check of the surrogate data using linear mutual information $L(X(t);Y(t+\tau))$ (a),(c). See caption of Fig. 3 for the line key.

5. The annual cycle is removed and there is a weak but long-term dependence apparent between the present $[X(t)]$ and the future $[X(t+\tau)]$ values of the studied series. Again, both linear and nonlinear statistics show significant differences from the surrogate data. It is time to consider a more sophisticated construction of surrogate data than just the simple phase randomization and fast Fourier transform as above. In order to avoid possible problems due to resampling we returned to the raw data and applied the method of Schreiber and Schmitz [9]. In this approach, surrogate data of unevenly sampled series are constructed using the Lomb periodogram and a combinatorial optimization for its inversion. No significant results, i.e., no evidence for nonlinearity, were found in the studied data.

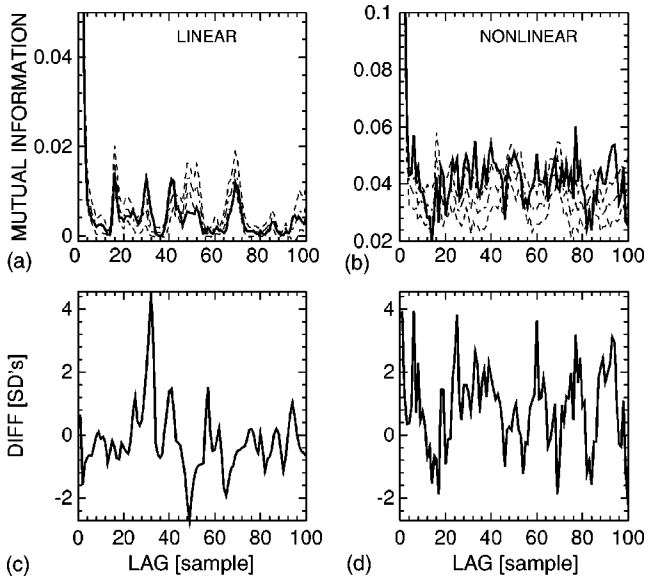

FIG. 5. Testing for nonlinearity in the residuals of the triple linear regression of the detrended unstable dilatometric time series on the meteorological variables, using mutual information $I(X(t);X(t+\tau))$ (b),(d) and the check of the surrogate data using linear mutual information $L(X(t);X(t+\tau))$ (a),(c). See caption of Fig. 3 for the line key.

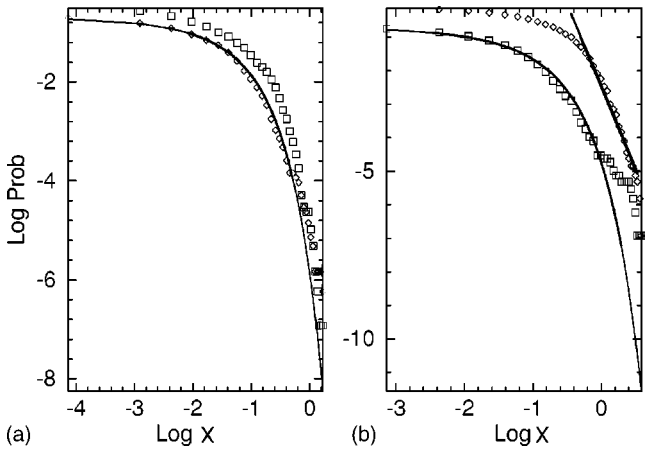

FIG. 6. The empirical probability $P(|x|>X)$ of observing amplitudes larger than a given value X (where x is a deviation from the mean value) for the triple regression residuals of an example of a stable (a) and unstable (b) time series of dilatometric measurements. Diamonds and squares illustrate left and right sides of the distribution. The solid line shows the average distribution of 10^5 realizations of a 1024-sample time series randomly drawn from the Gaussian distribution with the same mean and variance as the residuals under study.

Summing up the above results, we can see that the dynamics of the dilatometric measurements of relative displacements on rock cracks is strongly modulated by the meteorological variables. Their influence, namely, that of the atmospheric temperature, is reflected in a complex but linear way. The inherent dynamics of the rock slopes, reflected in the residuals of the triple regressions is probably linear, but, especially in the cases of unstable slopes, cannot be explained by a (transformed) linear Gaussian process, used as the null hypothesis in the above nonlinearity tests. In the next section we will analyze properties of these residuals.

IV. DISTRIBUTIONS AND TEMPORAL CORRELATIONS

In order to study distributions of the residuals (obtained by the above-described multiple linear regressions) we first bin the data into 64 bins and construct their histograms. Then, by summing the bins from the tail to the mean value, we obtain the empirical probability $P(|x|>X)$ of observing amplitudes larger than a given value X (where x is a deviation from the mean value). The examples of $P(|x|>X)$ for a stable and unstable dilatometric series are presented in Figs. 6(a) and 6(b), respectively. The distributions are asymmetric, with a small digression from the Gaussian distribution in the

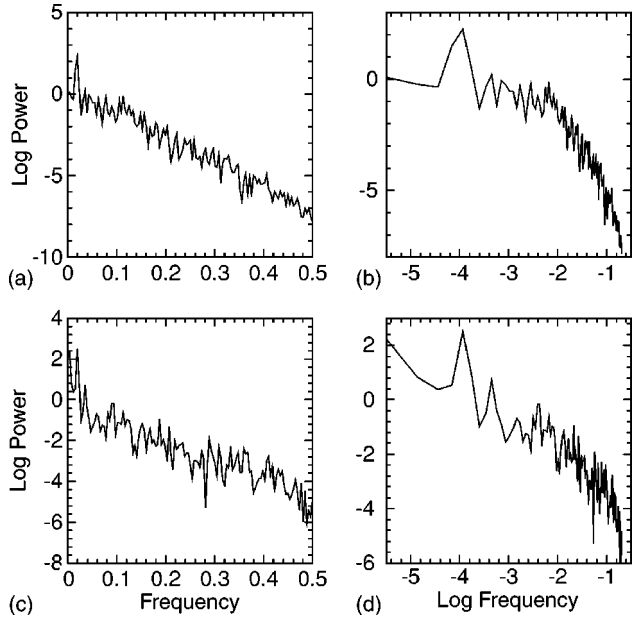

FIG. 7. Power spectra of regression residuals of an example of stable (a),(b) and of unstable (c),(d) time series of dilatometric measurements. Single (a),(c) and double (b),(d) logarithmic plots.

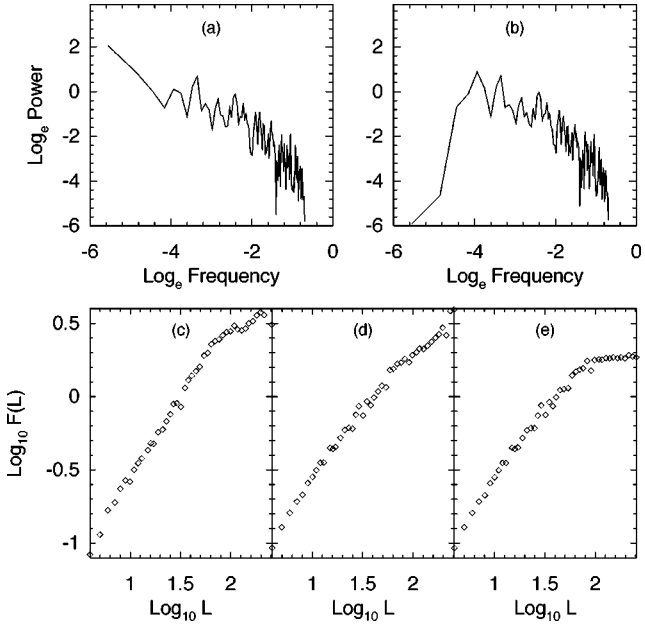

FIG. 8. Power spectra (a),(b) and results of the detrended fluctuation analysis (c)-(e) for the residuals of the single (c) and triple (a),(d) regressions of the linearly detrended time series of dilatometric measurements on an unstable slope; and of the triple regression of the high-pass filtered unstable dilatometric series (b),(e).

stable case [Fig. 6(a)]. For the unstable series [Fig. 6(b)] one tail is much "fatter" than the Gaussian distribution, i.e., large fluctuations are more likely to occur than the Gaussian distribution would predict. Moreover, this tail is consistent with a power law $P(|x|>X)\approx X^{-\mu}$ showing the increasing reduction of probability for increasing amplitude of the fluctuations. The robust linear regression [16] fit yields an estimate $\mu=4.8$, which is well outside the range for stable Lévy distributions $(0<\mu<2)$ [17].

In order to study the dynamics and temporal correlations of the residuals we calculate their power spectra [8]. The examples for stable [Figs. 7(a) and 7(b)] and unstable [Figs. 7(c) and 7(d)] dilatometric data are plotted in single [logarithm of power against frequency, Figs. 7(a) and 7(c)] and double [logarithm of power against logarithm of frequency, Figs. 7(b) and 7(d)] logarithmic plots. The power spectrum of the stable series [Figs. 7(a) and 7(b)] decays in a linear fashion in the case of the single logarithmic plot [Fig. 7(a)], i.e., the spectral power $S(f)$ as a function of the frequency f is best described by an exponentially decreasing curve $S(f)\approx\exp(-\gamma f)$. Such a power spectrum is typical for series with short-range correlations, i.e., the correlation function exponentially decreases with increasing time lag. The behavior of the spectrum of the unstable series is different—now an approximately linear decrease can be seen in the double logarithmic plot [Fig. 7(d)]. This spectrum is best approximated by a power-law decay $S(f)\approx f^{-\beta}$. The robust linear regression fit over the whole spectrum yields an estimate $\beta=1.5\pm0.6$. Such a power spectrum is a characteristic of fractal Brownian motion with long-term power-law correlations.

In addition to scaling of the distribution of fluctuations and of the distribution of energy over the power spectrum, we also study a possible scaling of fluctuations in their temporal evolution using so-called detrended fluctuation analysis (DFA) [7].

Briefly, for performing the DFA, the time series $\{x(i), i=1,\ldots,N\}$ is centered by subtracting its mean value $\overline{x}$ and integrated. The integrated time series $y(k)=\Sigma_{i=1}^{k}[x(i)-\overline{x}]$ is divided into boxes of equal length L. In each box of length L, a least squares line is fitted to the data (representing the trend in that box). The y coordinate of the straight line segments is denoted by $y_L(k)$. Next, we detrend the integrated time series $y(k)$ by subtracting the local trend $y_L(k)$ in each box. The root-mean-square fluctuation of this integrated and detrended time series is calculated using

$$F(L)=\sqrt{\frac{1}{N}\sum_{k=1}^{N}[y(k)-y_L(k)]^2}. \tag{1}$$

This computation is repeated over all time scales (box sizes L) to characterize the average fluctuation $F(L)$ as a function of box size L. Typically, $F(L)$ will increase with box size L. A linear relationship on a double logarithmic plot indicates the presence of power-law (fractal) scaling. Under such conditions, the fluctuations can be characterized by a scaling exponent α, the slope of the line relating $\log_{10}F(L)$ to $\log_{10}L$.

The DFA results obtained for the residuals of the linearly detrended unstable dilatometric series, obtained from the single multivariate linear regression on the meteorological variables, are presented in Fig. 8(c). [The related power spectrum was illustrated in Fig. 7(d)]. The long range of the linearly increasing dependence in the double logarithmic plot [Fig. 8(c)] confirms the presence of nontrivial long-term correlations and scaling of the fluctuation variance as $F(L)\approx L^{\alpha}$. In order to test this behavior in the residuals of the dilatometric data after further processing, we apply both the

spectral analysis and DFA to the residuals after triple regressions with lagged temperatures [Fig. 8(a), power spectrum; Fig. 8(d), DFA] and to the triple regression residuals obtained from the high-pass filtered dilatometric series [Fig. 8(b), power spectrum; Fig. 8(e), DFA]. The triple regression only removed the rest of the annual peak [located at position about −4 in the logarithmic frequency scale, cf. Figs. 7(d) and 8(a)], and the high-pass filtering removed all slow frequencies well over the annual peak [Fig. 8(b)], otherwise the scaling behavior did not change. Looking at these results, it is probable that the slow fluctuations ("nonlinear trends" with periods larger than 1 yr) are not caused by external forces, but are a part of the same fractal fluctuations as those on higher frequencies.

Our main interest in this study is a distinction between the stable and unstable slopes, which has been found on a qualitative level. Thus, at this stage we do not need to obtain estimates of the scaling exponents α and β. It is appropriate, however, to check their consistency using their relation [18]

$$\beta = 2\alpha - 1. \tag{2}$$

Estimates of the fluctuation coefficient α range between 0.9 and 1.1, while the spectral decay coefficient β from the whole spectrum is approximately 1.5 with a large variance leading to the standard deviation equal to 0.6. More detailed study can find two different scaling regions in the power spectra [Figs. 7(d), 8(a), and 8(b)], with scaling $\beta \approx 2$ and β between 1.3 and 1.7 in the high- and low-frequency bands, respectively. Similarly, the DFA plots yield the scaling coefficients $\alpha = 0.9$ and $\alpha = 1.1$ for the low- and high-frequency regions, respectively. Although the variance of the spectral estimates is very high, there seems to be an inconsistency with respect to relation (2). It can, however, be related to the finding of Malamud and Turcotte [19] that for time series of limited length, as in our case, the relation (2) holds only for $-1 < \beta < 1$. Still we have a possibility of checking the consistency of the scaling exponents using the knowledge that, for self-affine series, their integration increases the spectral decay coefficient by 2; and vice versa, derivation shifts β to $\beta - 2$ [19]. Therefore we construct differenced series from both types of residuals (of the single multivariate regression and the triple regression with the lagged temperatures) and plot their power spectra and DFA results in Fig. 9. This operation also made a sharp distinction between the two different scaling regions in both the power spectra [Figs. 9(a) and 9(b)] and the DFA results [Figs. 9(c) and 9(d)]. The high-frequency scaling region starts at periods of approximately four weeks. [29.5 days; 0.699 in the decadic logarithmic ($\log_{10}$) scale, which corresponds $L = 5$ samples. The irregularly sampled series representing 6026 days was regularly resampled into 1024 samples, thus giving the time 5.885 days per sample.] The region ends at the period of 11 weeks [76.5 days, 13 samples, or 1.114 in the DFA $\log_{10}$ scale in Figs. 9(c) and 9(d)]. This is consistent with the finding in the power spectra [Figs. 9(a) and 9(b)] where the scaling changes at the point −2.549 [natural logarithm ($\log_e$) scale]. This gives the frequency 0.078 cycle/sample, or a period of 12.79 samples. The low-frequency scaling region spans periods of about 580 days (ending shortly before 2 in the $\log_{10}$

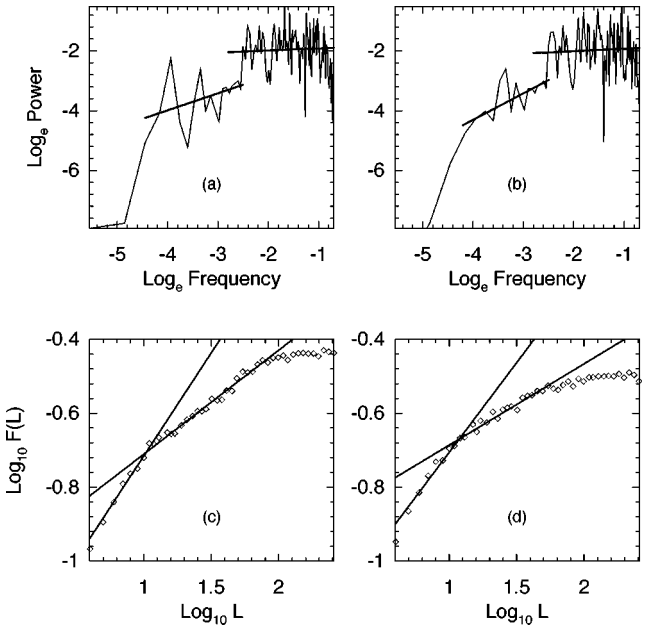

FIG. 9. Power spectra (a),(b) and results of the detrended fluctuation analysis (c),(d) for the differenced residuals of the single (a),(c) and triple (b),(d) regression of the linearly detrended time series of dilatometric measurements on an unstable slope. Thin curves in (a),(b) and points in (c),(d) are the results of the respective methods; thick solid lines in all figures are fitted robust linear regressions in particular scaling regions.

DFA scale or about −4.6 in the $\log_e$ frequency scale). The scaling exponents obtained by the robust linear regression are $\beta_1 = -0.57 \pm 0.5$ and $\beta_2 = -0.07 \pm 0.5$, $\alpha_1 = 0.28 \pm 0.01$ and $\alpha_2 = 0.55 \pm 0.01$, for the low- and high-frequency regions, respectively, for the differenced residuals of the single multivariate linear regression [Figs. 9(a) and 9(c)]. The results for the differenced residuals of the triple regression [Figs. 9(b) and 9(d)] are $\beta_1 = -0.8 \pm 0.4$ and $\beta_2 = -0.09 \pm 0.6$, $\alpha_1 = 0.22 \pm 0.01$ and $\alpha_2 = 0.49 \pm 0.01$. The results from other dilatometric series from unstable slopes are very similar. The related scaling exponents α and β are, within the variance of their estimates, consistent according to relation (2).

V. DISCUSSION AND CONCLUSION

Complex hierarchical patterns observed in long-term slope movement monitoring records [3–5] might resemble an evolution of a nonlinear system with a chaotic attractor. The necessary condition for the hypothesis of deterministic chaos is nonlinearity of the system under study. Our thorough analysis of time series of dilatometric measurements on rock cracks, representing the slope movements, did not, however, show any evidence for nonlinearity either in the intrinsic slope dynamics or in their relations to the dynamics of meteorological variables (atmospheric temperature, humidity, and precipitation). The atmospheric variability and seasonality has a strong influence on the slope dynamics and is reflected in the dilatometric series in a nontrivial, but linear, way. In particular, at least two delay mechanisms are present, that is, the temperature annual cycle can be regressed onto

the dilatometric series with one zero and two nonzero time lags. The residuals obtained from the dilatometric series by removing the meteorological influences are asymmetrically distributed fat-tailed non-Gaussian fluctuations with short-range correlations in the case of stable slopes. The distributions of the residuals obtained from the dilatometric measurements on unstable slopes are, on their "fatter" side, characterized by an asymptotic power-law distribution with decay coefficients between 4 and 5, i.e., outside the range of stable Lévy distributions $(0<\mu<2)$ [17]. When the fluctuations are of this type, the dynamics is intermittent and high-order moments diverge. Further, the dynamics of the unstable slopes possesses persistent long-range correlations of self-affine processes. Two scaling regions have been identified consistently by both the spectral analysis and the detrended fluctuation analysis. On time scales between 4 and 11 weeks the persistence is characterized by the spectral decay coefficient $\beta \approx 2$ which corresponds to a Brownian motion. Time scales from 11 weeks to almost two years are described by the spectral decay coefficient $\beta \approx 1.5$, which corresponds to a fractional Brownian motion.

Fluctuations with hyperbolic intermittency and scaling spectra are expected to occur due to the action of cascade processes transferring energy from large to small scales [17]. This finding could support the proposal of Zvelebil [4,5] to model the dynamics of a rock slope collapse preparation by a hierarchically structured, complex nonequilibrium system which might show at least two different types of behavior on two different scaling ranges. From the practical point of view, however, the most promising result is the qualitative difference found between the types of correlation decay in the dynamics of stable and unstable slopes (Fig. 7). Nevertheless, the preliminary character of this result should not be neglected and further studies are necessary before any generalization. It should be established how a particular geometry and geology of a slope determine the slope dynamics and under which conditions the fractal dynamics can serve as a precursor of instability. The other interesting question is whether the observed scaling propagates also onto shorter time scales. Therefore, it is desirable to analyze higher-frequency data than those used in this study. In the case of a positive answer, engineering geology could obtain a powerful tool for assessing the stability of rock slopes from a relatively short-term monitoring of the slope dynamics.

ACKNOWLEDGMENTS

The authors would like to thank Professor P. V. E. McClintock for careful reading of the manuscript. The study was supported by the Grant Agency of the Czech Republic (Project No. 205/00/1055).

[1] L. Bjerrum and F. Jorstad, Norges Geotekniska Institutt Publ. (Oslo) **79**, 1 (1968).
[2] J. Zvelebil and M. Moser, Phys. Chem. Earth B, **26**, 159 (2001).
[3] J. Zvelebil, Acta Univ. Carol. Geogr. **1995**, 79 (1995).
[4] J. Zvelebil, in *Landslides*, edited by K. Senneset (Balkema, Rotterdam, 1996), pp. 1473–1480.
[5] J. Zvelebil, Ann. Geophys. **16** Supp. IV, NP1, 1082 (1998).
[6] S. Qin, J. J. Jiao, and S. Wang, Geomorphology **43**, 77 (2002).
[7] C.-K. Peng, S. V. Buldyrev, S. Havlin, M. Simons, H. E. Stanley, and A. L. Goldberger, Phys. Rev. E **49**, 1685 (1994); C.-K. Peng, S. Havlin, H. E. Stanley, and A. L. Goldberger, Chaos **5**, 82 (1995); software available at www.physionet.org, see A. L. Goldberger, L. A. N. Amaral, L. Glass, J. M. Hausdorff, P. Ch. Ivanov, R. G. Mark, J. E. Mietus, G. B. Moody, C.-K. Peng, and H. E. Stanley, Circulation **101**, e215 (2000).
[8] The DATAPLORE software package (www.datan.de) was used for resampling, detrending, filtering, linear regressions, and spectral analyses.
[9] T. Schreiber and A. Schmitz, Phys. Rev. E **59**, 409 (1999). The routine randomize_uneven can be obtained from http://www.mpipks-dresden.mpg.de/~tisean/.
[10] M. Paluš, Physica D **80**, 180 (1995).
[11] M. Paluš, Phys. Lett. A **213**, 138 (1996).
[12] T. M. Cover and J. A. Thomas, *Elements of Information Theory* (J. Wiley & Sons, New York, 1991).
[13] J. Theiler, S. Eubank, A. Longtin, B. Galdrikian, and J. D. Farmer, Physica D **58**, 77 (1992).
[14] D. Prichard and J. Theiler, Phys. Rev. Lett. **73**. 951 (1994).
[15] T. Schreiber and A. Schmitz, Physica D **142**, 346 (2000).
[16] W. H. Press, B. P. Flannery, S. A. Teukolsky, and W. T. Vetterling, *Numerical Recipes: The Art of Scientific Computing* (Cambridge University Press, Cambridge, U.K., 1986)
[17] *Non-Linear Variability in Geophysics. Scaling and Fractals*, edited by D. Schertzer and S. Lovejoy (Kluwer, Dordrecht, 1991).
[18] S. Havlin, R. B. Selinger, M. Schwartz, H. E. Stanley, and A. Bunde, Phys. Rev. Lett. **61**, 1438 (1988).
[19] B. D. Malamud and D. L. Turcotte, J. Stat. Plan. Infer. **80**, 173 (1999).